Nanocomposites of ZnO/CuO/Se Synthesized by *Schinus terebinthifolia* Biomass and their Antioxidant, Cytotoxicity, Anti-*H. pylori*, and Anti-obesity Properties

Mohanned T. Alharbi [a], Aisha M. H. Al-Rajhi [b,*], Mohammed S. Almuhayawi [c,d], Hattan S. Gattan [e,f], Mohammed H. Alruhaili [c,f], Yahya Ali [g], and Samy Selim [h]

A watery extract of *Schinus terebinthifolia* leaves was used as the source for producing a nanocomposite of ZnO/CuO/Se (NC ZnO/CuO/Se). Transmission electron microscopy (TEM), UV, X-ray diffraction, and scanning electron microscopy-energy were employed to characterize NC ZnO/CuO/Se. Based on the TEM investigation, the nanoparticles had an average size between 40.9 and 50.2 nm. NC ZnO/CuO/Se had potent anti-*H. pylori* activity, as evidenced by a zone of inhibition of 34.3 mm. The NC ZnO/CuO/Se successfully inhibited *H. pylori* (MIC = 15.6 µg/mL) and showed better antimicrobial activity in comparison with the control. At 75% of MBC, it dramatically decreased the production of bacterial biofilms (91.1% inhibition). High antioxidant qualities were demonstrated by the NC ZnO/CuO/Se (> 88% in the DPPH assay). It demonstrated outstanding enzyme inhibition capacity against lipase, with an IC_{50} of 41.66 ug/mL. The IC_{50} value of NC ZnO/CuO/Se against normal cell lines (WI38) was 593.08 ± 2.35 µg mL^{-1}, which is a high dose. From the overall results, NC ZnO/CuO/Se exhibited favorable biological effects *in vitro* as a wide-spectrum treatment for various medical uses.

DOI: 10.15376/biores.20.2.4432-4449

Keywords: Nanocomposite; Schinus terebinthifolia; Anti-obesity; Antimicrobial activity

Contact information: a: Department of Basic Medical Sciences, College of Medicine, University of Jeddah, Jeddah, Saudi Arabia; b: Department of Biology, College of Science, Princess Nourah bint Abdulrahman University, P.O. Box 84428, Riyadh 11671, Saudi Arabia; c: Department of Clinical Microbiology and Immunology, Faculty of Medicine, King Abdulaziz University, Jeddah 21589, Saudi Arabia; d: Yousef Abdulatif Jameel Scientific Chair of Prophetic Medicine Application, Faculty of Medicine, King Abdulaziz University, Jeddah 21589, Saudi Arabia; e: Department of Medical Laboratory Technology, Faculty of Applied Medical Sciences, King Abdulaziz University, Jeddah 21589, Saudi Arabia; f: Special Infectious Agents Unit, King Fahad Medical Research Center, King AbdulAziz University, Jeddah, Saudi Arabia; g: Department of Biology, College of Science, Jazan University, P.O. Box 114, Jazan 45142, Saudi Arabia; h: Department of Clinical Laboratory Sciences, College of Applied Medical Sciences, Jouf University, Sakaka 72388, Saudi Arabia;
**Corresponding author: amoalrajhi@pnu.edu.sa*

INTRODUCTION

One of the most exciting and inventive disciplines in science and technology, nanotechnology, has many uses in different applications from engineering, energy, electronics, dye degradation, agriculture, and medicine (Yahya *et al.* 2022; Al-Rajhi and Abdelghany 2023a; Qanash *et al*. 2023a; Revathi *et al*. 2024; Idris *et al*. 2025). These nanoscale materials have been created using various techniques, including physical,

chemical, and green approaches (Al-Rajhi and Abdelghany 2023b; Qanash *et al*. 2023a), but each has many disadvantages. Conventional physical and chemical techniques for synthesizing metal nanoparticles are increasingly considered obsolete due to their intricate manufacturing processes, elevated energy requirements, and the generation of hazardous by-products that present significant hazards to health of human and the environment (Singh *et al.* 2024).

In recent decades, green technologies have been the favored method for generating nanoparticles (NPs) or nanocomposites (NCs) because of their cost-effectiveness, safety, low environmental impact, and biocompatibility, distinguishing them from alternatives. Owing to their diminutive size and extensive exterior area, NPs comprised of metal compounds possess a diverse array of applications (El-Batal *et al*. 2023; Amin *et al*. 2024; Soliman *et al*. 2024; Selim *et al.* 2025; Michael *et al*. 2024). NCs comprising three metals or metal compounds have shown exceptional features, including high stability, enhanced sensitivity and selectivity, and a range of shapes and sizes relative to surface area. These attributes contribute to their promising catalytic activity, antimicrobial properties, photocatalytic potential, drug delivery capabilities, biosensor functionality, and various biotechnological and biotherapeutic utilizations when compared to single and dual metal compound alternatives (Salama *et al*. 2021).

In the current study, aqueous extract from *Schinus terebinthifolia* leaves was used as a reducing agent to create NC ZnO/CuO/Se. The extract is known to contain many bioactive components such as phenolic and flavonoids (da Silva Nascimento *et al*. 2023).

Most people globally can become infected with *Helicobacter pylori*, which can have dangerous health effects. *H. pylori* is the most common cause of gastritis (Hooi *et al.* 2017; Bakri *et al.* 2022; Al-Rajhi *et al.* 2023a,b). Additionally, intestinal-type gastric cancer and dysplasia are linked to gastric atrophic necrosis (GAD), which is caused by chronically produced gastritis (Shirani *et al*. 2023). *Helicobacter pylori* is the main causative agent connected to several diseases, such as inflammation and the emergence of stomach ulcers (Shehab *et al*. 2024). There is still no 100% effective treatment for *H. pylori*, despite its discovery almost 40 years ago (Sasaki *et al*. 2021).

The issue of obesity has been around for a long time. In addition to causing cosmetic issues, obesity also leads to an incorrect biological metabolism, which results in several physiological and psychological and societal issues. One significant danger factor for conditions like heart illness is obesity, increasing blood pressure, raised cholesterol levels, and even cancer, and it is intimately linked to the development of numerous chronic illnesses (Bjerregaard *et al*. 2018). Lipases are members of the hydrolases family of enzymes that are specifically designed to catalyze the lysis of triacylglycerol (TAG) ester bonds, resulting in the production of glycerol and free fatty acids (Fahim *et al.* 2024). Lipids, such as triglycerides, are reduced by the lipase inhibitors, which work to control and treat obesity by combining with the active lipase portion found in the stomach and small intestine to change the stomach/trypsin structure, restrict catalytic activity, and reduce the digestion and absorption of lipids in food. Additionally, the hydrolysis contributes to the accumulation of adipose tissue (Sánchez *et al*. 2008). Most studies concentrate on mono- or bimetallic NPs, but little work has been done on biogenic NC ZnO/CuO/Se. Consequently, the novelty of this study examines how *Schinus terebinthifolia* leaves aqueous extract produced NC ZnO/CuO/Se and showed the

important role of these NC in the treatment of *H. pylori* and obesity problems for the first time with reference to their antioxidant and cytotoxicity properties.

EXPERIMENTAL

Bio-fabrication of NC ZnO/CuO/Se

The *Schinus terebinthifolia* leaves were collected from the garden of the Jouf University, Saudi Arabia, cleaned three times with tap water to remove any impurities, and then allowed to air dry before being ground. The resulting leaf powder was combined with distilled H_2O (10 g/100 mL) and agitated for 60 min at 150 rpm. The combination was then centrifuged to produce a clear supernatant, which catalyzed the creation of NC ZnO/CuO/Se. To synthesize NC ZnO/CuO/Se, a 10 mM solution of every metal (Na_2SeO_3, $ZnSO_4 \cdot 2H2O$, and $CuSO4 \cdot 2H_2O$) was combined in a 1:1:1 ratio with the leaves aqueous extract at a 4:1 volume ratio. The alkali condition (pH 8) was rectified by employing NaOH and stirring at 65 °C for 2 h. The reduction of metal precursors using fruit extract to synthesize nanoparticles was signified by a reddish-brown hue (Amin *et al*. 2025). Subsequent to the evaporation of the synthetic solution and rinsing with deionized water followed by alcohol to eliminate impurities, the residual material was collected. The resultant residue was subsequently hardened for 60 min at 200 °C to provide powder with reddish-brown color, which was then stored in a falcon tube for subsequent processes.

NC ZnO/CuO/Se Characterizations

The diverse chemical groups in the extract of plant were characterized by means of Fourier transform infrared spectroscopy (FTIR, -Cary-630- Tokyo, Japan), resulting in the production of NPs. A JEOL-1010 transmission electron microscope was employed to ascertain the morphological features (dimensions and shapes) of the synthesized nanoparticles. The JSM6360LA energy dispersive X-ray diffraction (SEM-EDX, JEOL, Japan) was employed to analyze the surface morphology and chemical composition of nanoparticles for further exploration.

Preparation of Bacterial Suspensions

The *H. pylori* strain was obtained as a clinical specimen from Ain Shams Hospital. The VITEK® 2 Portable system was used to identify the strain, and VITEK® MS at 57357 Hospital verified the identification. Microorganism colonies were moved to tubes with sterilized physiologically appropriate solution of saline, and the turbidity was modified to the standard of 2.0 McFarland (Abdelghany *et al*. 2023a). The suspension created by this turbidity is equivalent to about 1.0 x 10^8 CFU/mL of *H. pylori*.

Determination of anti-*H. pylori* Activity

Anti-*H. pylori* property *in vitro* was measured using the well diffusion of agar method (Castillo-Juárez *et al*. 2007). In summary, 100 µL of *H. pylori* suspensions (1.0 × 10^8 CFUs/mL) was applied to Mueller Hinton agar dishes augmented with 10% blood of sheep. A hole with a diameter of 6 mm was precisely punched employing a sterilized cork borer. Subsequently, 100 µL of the NC ZnO/CuO/Se or an antibiotic at the designated quantity was injected to the well. Metronidazole (MTZ, 0.8 mg/mL), amoxicillin (AMX,

0.05 mg/mL), and clarithromycin (CLR, 0.05 mg/mL) were utilized for the positive, whereas DMSO functioned as a negative controls. The diameter of the inhibitory zone was measured after a 72-h incubation at 37 °C.

Minimal Inhibitory Concentration (MIC) and Anti-biofilm

The micro-dilution broth technique, utilizing Mueller-Hinton broth combined with lysed blood of horse, enabled the calculation of the MIC of the subjected NC ZnO/CuO/Se. The amount of the investigated nanoparticles ranged from 0.98 to 1000 µg/mL and were accomplished through serial two-fold dilutions. For the preparation of sterile 96-well polystyrene microtitrate plates (PMP), 200 µL of a diluted NC ZnO/CuO/Se in broth medium was added to each well. The microbiological cultures were prepared as inocula in 0.85% NaCl to achieve the turbidity specified by the 1.0 McFarland standard. Two µL were added to each well to obtain a final density of 3.0×10^6 CFU (colony-forming units) per mL. The MICs were determined as the minimum concentration of the sample that exhibited complete inhibition of growth of the reference strain after a 72-h incubation at 35 °C in a microaerophilic environment with 15% CO_2. Each microplate included a negative control comprising the test nanoparticles without bacteria and a positive control containing inoculum absent of the tested nanoparticles (Malm *et al.* 2015). The minimum bactericidal concentration (MBC) was established by subculturing 100 mL of the microbial culture from each well exhibiting complete growth inhibition, as well as from the last positive well and the growth control, onto Mueller-Hinton agar plates supplemented with 10% sheep blood. The plates were incubated at 35 °C for 72-h under microaerophilic environments, with the minimum bactericidal concentration (MBC) defined as the lowest extract concentration of NPs that inhibited microbial growth. The MBC/MIC ratios were computed to assess the bactericidal or bacteriostatic effects of the tested extracts. In this research, antibacterial agents were classified as bactericidal when the ratio of MBC to MIC did not exceed four times the MIC (French 2006).

Biofilm formation in PMP was examined to detect NC ZNO/CUO/SE effects (Alghonaim *et al.* 2024). In the technique, 300 µL of freshly prepared trypticase soy yeast broth (TSY) inoculated (10^6 CFU/mL) was aliquoted into every PMP well and cultured at predefined sublethal doses (75, 50, and 25% MBC). Control wells had medium, methanol, and no NC ZnO/CuO/Se. Plates were incubated at 37 °C for 48 h. After incubation, the supernatant was discarded and every well was washed with sterilized distilled water to remove free-floating cells. The biofilm was dyed with 0.1% crystal violet in H_2O for 15 min after the plates air-dried for 30 min. Washing the plate three times with sterile distilled H_2O to detach excess stain after incubation. To dissolve the dye on the cells, 250 µL of 95% ethanol was added to each well after 15 min of incubation. The absorbance (AB) of the sample has been determined with a 570 nm microplate reader (Selim *et al*. 2004).

$$\text{Biofilm inhibition (\%)} = 1 - \frac{\text{AB of NC ZNO/CUO/SE} - \text{AB of blank}}{\text{AB of control} - \text{AB of blank}} \text{ x } 100 \qquad (1)$$

DPPH Assessment

NC ZNO/CUO/SE were evaluated for DPPH sequestration by dispersing double-fold levels (1.95 to 1000µg mL^{-1}) in Milli Q H_2O, while DPPH could be dissolved in methanol. In a test tube, 1.0 mL for each quantity, DPPH, and 450 µL of Tris-HcL buffer (pH = 7.4) were mixed. After mixing, the mix was agitated (150 rpm) in a dark 37 °C

atmosphere for 30 min. Ascorbic acid was the positive control while NC ZnO/CuO/Se or a test tube without them was the negative control (Al-Rajhi *et al*. 2022). The percentages were computed after the scavenging activity by spectrophotometrically at 517 nm was detected as follows:

$$\text{Scavenging (\%)} = \frac{\text{AB of control} - \text{AB of test}}{\text{AB of control}} \text{ x } 100 \quad (2)$$

Cytotoxicity of NC ZNO/CUO/SE

Using the MTT assay technique, the cytotoxicity of NC ZnO/CuO/Se was examined against normal human lung cell lines (Wi38). These cells were acquired from Cairo, Egypt's Vaccines Company (VACSERA). The selected normal cell was cultured in PMP until it reached 1 x 10^5 cells per 100 µL per well. It then spent a day in a 5% CO_2 incubator at 37 °C. After creating a monolayer sheet, 100 µL of RPIM medium was applied. The mixture was incubated at 37 °C for 48 h after adding NC ZnO/CuO/Se at concentrations ranging from 1000 to 31.25 µg mL^{-1}. The control wells were three DMSO-treated wells. The MTT solution (50 µL, 5 mg mL^{-1} phosphate buffer) was applied to cells after 48 h, after removing excess media. After mixing well, they were incubated at 37 °C for 5 h. The formazan crystal formed during MTT catabolism was dispersed by adding 100 µL of 10% DMSO to each well after removing the excess MTT solution. The color AB at 570 nm was measured after 30 min without DMSO. Cell viability percentages were calculated using this formula (Abdelghany *et al*. 2023b):

$$\text{Viability percentages (\%)} = \frac{\text{AB of treated cells}}{\text{AB of control}} \text{ x } 100 \quad (3)$$

Lipase Inhibition Assay

A solution of lipase was prepared by gently combining 10 mg of the lipase with 10 mL of buffer solution (1 mg/mL) immediately before use. NC ZnO/CuO/Se was synthesized at identical amounts. Lipase activity was evaluated using p-nitrophenyl butyrate (PNPB) as a substrate. Lipase stock solutions (1 mg/mL) were prepared in 0.1 mM potassium phosphate buffer (PPB) pH 6.0) and stored at -20° C. Before assessing lipase inhibitory action, lipase was preincubated for 1 h at 30 °C in a PPB (0.1 mM, pH 7.2, 0.1% polysorbate 80, Tween 80) alongside NC ZnO/CuO/Se (7.8, 15.62, 31.25, 62.5, 125, 250, 500, and 1000 µg/mL) or Orlistat (at equivalent doses) as a standard control. Subsequently, 0.1 µL of pNPB was used as a substrate to initiate the reaction, resulting in a total volume of 100 µL.

A Biosystem 310-plus UV-Visible spectrophotometer (JASCO V-560) was employed to quantify the concentration of p-nitrophenol generated in the reaction at 405 nm over a 5-min incubation time at 30 °C. The activity of the negative control was examined both in the presence and absence of an inhibitor (Roh and Jung 2012). The inhibitory capacity was assessed using the subsequent formula:

$$\text{Lipase inhibition (\%)} = 100 - \frac{B-b}{A-a} \times 100 \quad (4)$$

The absorbance of the activity of lipase with inhibitor is designated as *B*, the absorbance of the negative control (NC ZnO/CuO/Se in DMSO) with inhibitor alongside no lipase is designated as *b*, the absorbance of lipase activity without inhibitor is designated

as *A*, and the absorbance of negative control (DMSO) without inhibitor and without lipase is designated as *a*.

Statistical Analysis

The Minitab 19 program (Minitab LLC, State College, PA, USA) was utilized to generate the statistical assessment, and *post hoc* evaluations were directed *via* Tukey's test (honest significant difference), through a significance level of $p < 0.05$.

RESULTS AND DISCUSSION

Characterization of NC ZnO/CuO/Se

The extract of *S. terebinthifolia* succeeded as a mediator in the synthesis of NC ZnO/CuO/Se. The three metals in the NPs form were joined together as a NC and enclosed by the extract matrix. Morphological features, such as sizes and forms that were identified by TEM research, are the primary factors influencing the use of nanoparticles as well as nanocomposites. The TEM images in Fig. 1 display the spherical and hemispherical shape of NC ZnO/CuO/Se. The size of NC ZnO/CuO/Se ranged from 40 to 50 nm (Fig. 1A). The findings that were observed were not consistent with the successful synthesis of NC ZnO/CuO/Se utilizing the strain of fungi *Aspergillus niger*, which had a size of 26.3 nm and a tetragonal pyramid shape (Hashem *et al*. 2023). The authors of a different investigation on green NC ZnO/CuO/Se made from *Nitraria retusa* aqueous extract demonstrated the development of spherical and crystallographic NC ZnO/CuO/Se with a size mean of 47.69 nm (Amin *et al*. 2025). When it comes to detecting the crystalline phase of formed nanoscale ingredients, the electron microscopy practice recognized as designated area electron diffraction (SAED) is useful. Eight distinct and crisp rings that represent the crystallographic properties of the constituent materials (ZnO, CuO, and Se) were apparent in the SAED image of the NC ZnO/CuO/Se (Fig. 1B). This information was compared to a SAED image of ZnO/CuO/Se produced by fungi, which revealed eight rings that give components their crystalline structure. The size and construction of NPs have an impact on their activity within live cells (He *et al*. 2010). They found that the size and form of the cells affect their diffusion, distribution, and response to NPs.

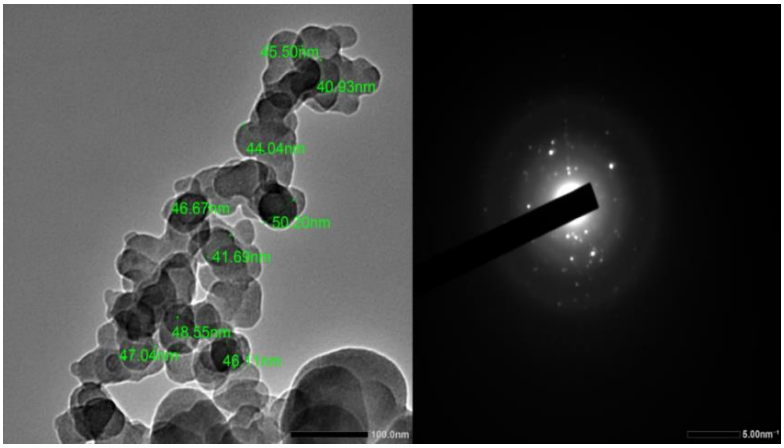

Fig. 1. TEM and SAED images of NC ZnO/CuO/Se NPs

Figure 2 displays the SEM images with a lower magnification, confirming that the metallic particles gathered into a conventional metal and metal oxide morphological appearance. The particle's appearance as compact layers with distinct borders and edges were another important characteristic. The many metals utilized in the biosynthesis may be the cause of this phenomenon. Using EDX analysis, the elemental components of NC ZnO/CuO/Se were identified both quantitatively and qualitatively. The Cu, Zn, and Se ions were confirmed to be the principal constituents of the produced sample, as illustrated in Fig 2. The production of ZnO, CuO, and Se ion were shown by the peaks at bending energies of 1, 8.6 KeV, 8.1 KeV, and 2.3, 11.5 KeV, respectively. NC ZnO/CuO/Se's quantitative metal ratios were arranged in the following order (from high concentration to low concentration) based on the EDX analysis: According to Fig. 3, the atomic percentages of Se > Cu > Zn were 5.35, 3.69, and 3.18%, whereas the percentages of weight were 17.03, 9.44, and 8.36%, correspondingly. These results do not agree with Hashem *et al*. (2023), who reported that Zn had the highest metal concentration (9.03 weight %), followed by Cu and Se (2.63 and 1.63 weight percentages, respectively) of NC ZnO/CuO/Se produced by fungi. Adsorption of O from the surrounding environment on the surface of the nanoparticles or the synthesis of CuO and ZnO could be the origin of the high concentration of O ions (weight percentages of 34.5% and atomic percentages of 51.5%).

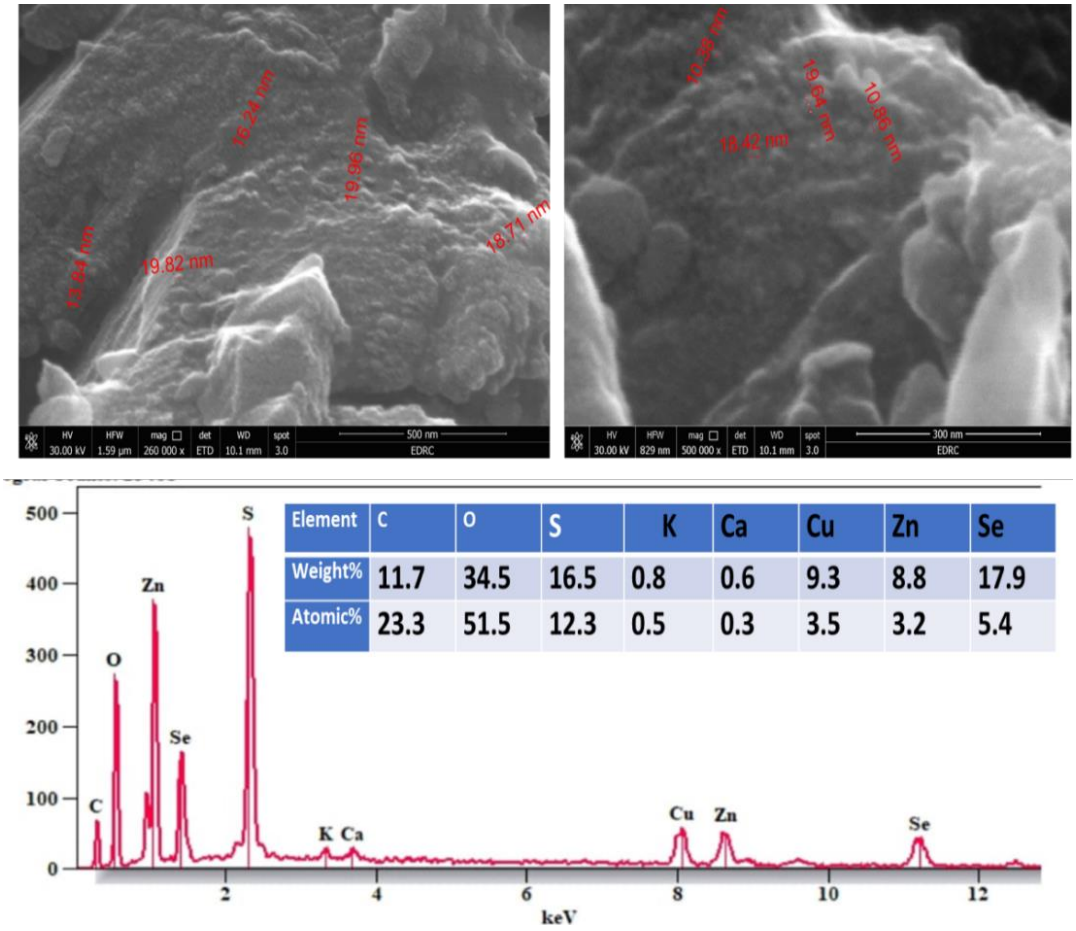

Fig. 2. SEM/EDX analysis revealing the metallic components of green-fabricated NC ZnO/CuO/Se

FTIR spectroscopy was used to examine how the active ingredient in the *Schinus terebinthifolia* leaves aqueous extract reduced different metals in a solution before capping NC ZnO/CuO/Se. The creation of the NC and the new appearance of functional groups caused the intensity of the preexisting peaks in the plant extract to rise or decrease. Six intense peaks were apparent at 3422, 2919, 2850, 1625, 1033, and 757 cm^{-1} in the plant extract. There were peaks located at wavenumbers 3432, 2962, 1605, 1352, 1115, 613, and 463 cm^{-1} following the synthesis of NPs. In addition to the emergence of new peaks following the reaction of extract with precursor of metal and metal oxide to generate NC ZnO/CuO/Se, these peaks' intensities were altered (Fig. 3).

The capping, reduction, and stabilization of NC ZnO/CuO/Se may be caused by several molecules namely carbohydrates, organic acids, proteins, amines, amino acids, and other ingredients, which may be linked to the presence of different purposeful groups in the extract of plant.

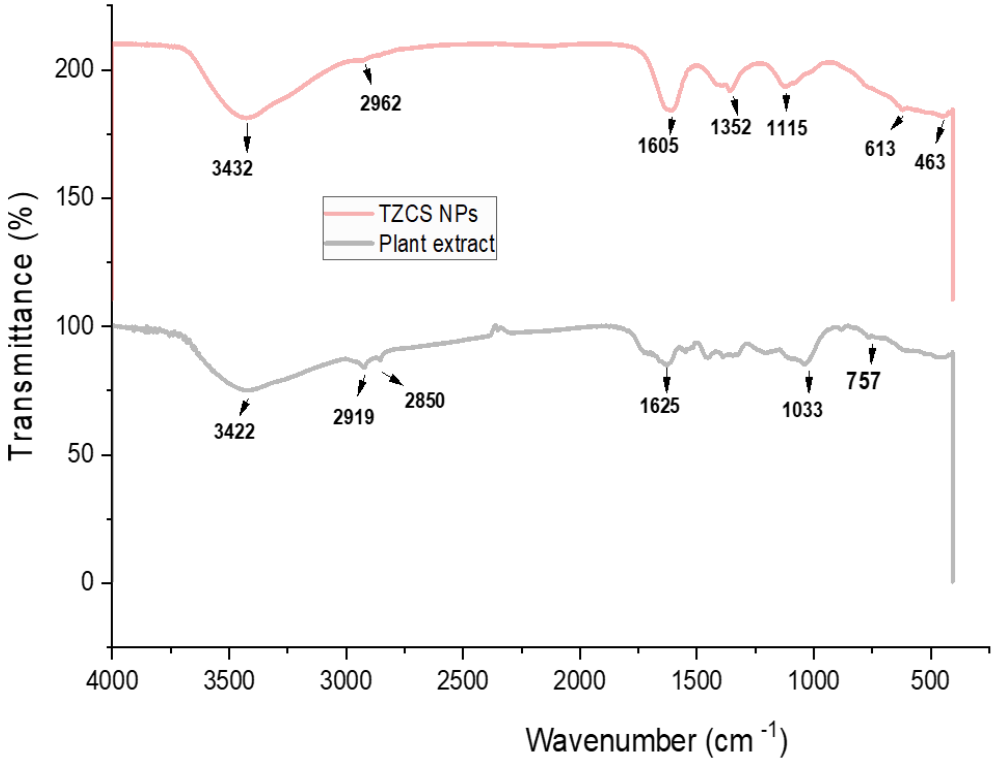

Fig. 3. NC ZnO/CuO/Se (TZCS NPs) and plant aqueous extracts with FTIR analysis displaying various functional groups

Figure (4a) illustrates the crystallographic arrangement of the NC ZnO/CuO/Se. The peak observed at 31.8° resulted from the interaction among the three nanoparticle integrations, exhibiting a notable intensity (Hasanin and Youssef 2022). Furthermore, the peak observed at 38.7° was likewise associated with integrating ZnONPs and CuONPs (Cao *et al*. 2021). In contrast, the peaks observed at 55.6°, 68.9°, and 72.6° corresponded to the presence of ZnO, CuO, and Se nanoparticles. As a result, the crystallographic diffraction pattern confirmed the simultaneous introgression of the three metals in nanoform exhibiting hexagonal characteristics.

UV–visible spectroscopy can yield valuable insights from this perspective. The UV–visible spectrum of the NC ZnO/CuO/Se is depicted in Fig.4 b, confirming the presence of the three nanometals. Notably, there were no conventional bands, but rather a series of peaks corresponding to each metal's characteristics. The bands observed at 355, 430 and 555 nm serve to affirm the presence of CuONPs, ZnONPs, and SeNPs, respectively; however, a precise recording was not attainable due to the overlapping of the bands (Surendra *et al.* 2021). The results obtained in this manner provide prospective confirmation of the biosynthesis and integration of the NC ZnO/CuO/Se structure.

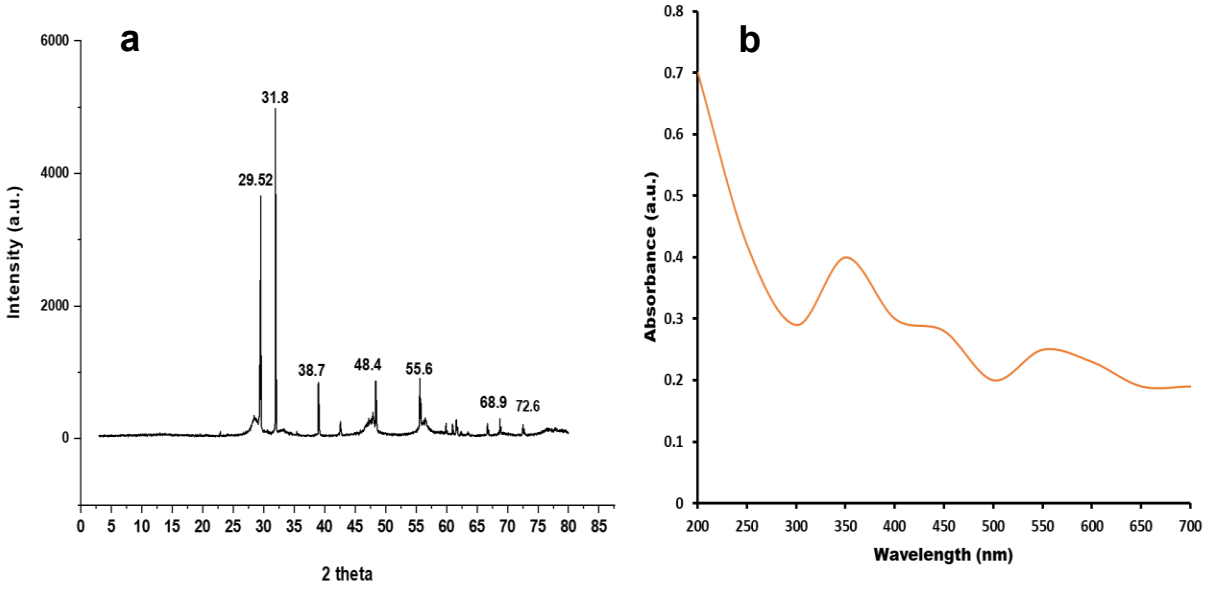

Fig. 4. The diffraction pattern of the NC ZnO/CuO/Se (a) and the UV–visible spectrum (b)

Antimicrobial and Antibiofilm Assay of NC ZnO/CuO/Se

Compared to NC of two metals, NC of three metals nanoparticles have shown effective and encouraging antibacterial properties (Nasrollahzadeh *et al*. 2020). The antimicrobial activity of NC ZnO/CuO/Se against *H. pylori* was evaluated for the first time in this study. The biosynthesized NC ZnO/CuO/Se exhibited potent antimicrobial activity against *H. pylori*, with an area of inhibition of 34.3 mm in comparison to the control of 24 mm (Table 1).

In a report on another NC, NC CuO/NiO/ZnO demonstrated strong antibacterial properties on *S. aureus* and *E. coli* bacteria; the NPs adhered to the bacterial cell wall and destroyed the cells (Paul *et al*. 2020). In a different investigation, the green-synthesized NC Au-Pt-Ag showed promise for anti-biofilm and antibacterial properties against *Candida albicans*, *S. aureus*, *E. coli*, *Enterococcus facial*, and *Enterococcus faecalis* (Dobrucka 2020). It was found that reactive oxygen species (ROS) cause cellular death, membrane alterations, a drop in ATP levels, and the blockage of tRNA binding to the ribosome are some of the key mechanisms for these nanomaterials' antibacterial effects.

The current study showed that the MIC and MBC of NC ZnO/CuO/Se against *H. pylori* was 15.62 µg/mL, compared to control 31.2 and 62.5, respectively (Table 1). The outcomes also displayed that the average percentage of biofilm formed in the presence of

3/4, 1/2, and 1/4 MBC of NC ZnO/CuO/Se was 91.1%, 79.7%, and 68.1%, respectively (Table 2).

A one-way ANOVA test was applied between the different NC ZnO/CuO/Se concentrations against the percentage of biofilm formed. At 3/4, 1/2, and 1/4 MBC levels, it differed significantly ($p < 0.05$). The MBC/MIC index of NC ZnO/CuO/Se recorded bactericidal properties, with every reading below 4.

Table 1. Inhibitions Zones, MIC, and MBC for *H. pylori* of Green-fabricated NC ZnO/CuO/Se

Treatment	Inhibition Zone (mm)	MIC (µg/mL)	MBC (µg/mL)	MBC/MIC Index
Control	24.0	31.25	62.5	2
NC ZNO/CUO/SE	34.3	15.62	15.62	1

Table 2. Activity of green-fabricated NC ZnO/CuO/Se at different doses of its MBC against biofilms *H. pylori*

NC ZnO/CuO/Se MBC% of *H. pylori*	Anti- Biofilm Activity (%)	
Media+Organism (Cont.)	-	
25% of MBC	68.12	
50% of MBC	79.71	
75% of MBC	91.14	

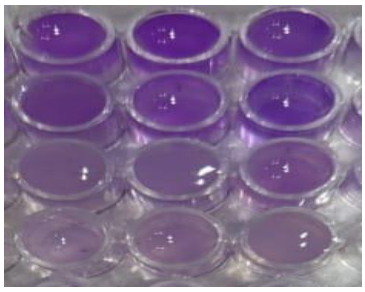

Antioxidant Activity

Free radicals, which are also described as ROS, are unstable molecules that are distinguished by their capacity to operate independently. In the human body, they are generated through oxidation processes or when cells are subjected to toxic environment or ingredients like radiation, pollutants, and other substances. This ROS has a detrimental effect on the constituents of cells, such as amino acids, DNA, and lipids (Peddi *et al*. 2021). Therefore, finding novel antioxidant compounds to counteract the harmful effects of ROS is essential. Here, the antioxidant capacity of the biogenic NC ZnO/CuO/Se was examined using a popular antioxidant assay: DPPH scavenging. The antioxidant values of NC ZnO/CuO/Se were estimated using DPPH scavenging (%) instead of ascorbic acid (Table 3). The DPPH radical efficiency increased dose-dependently from 16.4% to 88.5%, increasing NC ZnO/CuO/Se concentrations ranging from 1.95 to 1000 µg/mL. Another investigation on biogenic NC Cu/Ag/Zn found that at 1000, 500, and 50 µg mL^{-1}, the scavenging percentages were 68.3, 37.3, and 35.7% (Kunwar *et al.* 2023).

According to a report on NC ZnO/CuO/Se produced by *Nitraria retusa* extract, the maximal DPPH scavenging activity was achieved at 1000 µg mL^{-1}, which was lower than that of ascorbic acid, which was 98.3% (Amin *et al*. 2025). Due to the synergistic impact of multiple metals working together, several authors have shown that the scavenging activity of trimetallic nanoalloys is superior than that of single metal nanoparticles. For

example, applying the DPPH technique, the scavenging activity of Se-NPs produced by extract from *Cassia javanica* flowers was 82% at 1000 µg mL^{-1} with IC50 at 53.34 µg/L (Soliman *et al*. 2024). Additionally, ZnO-NPs made from *Limonium pruinosum* crude extract demonstrated 75.2% antioxidant activity at 1000 µg mL^{-1} (Naiel *et al*. 2022).

Table 3. DPPH Assessment of Green-fabricated NC ZnO/CuO/Se

Concentration (µg/mL)	DPPH Scavenging (%)		HSD at 0.05
	NC ZNO/CUO/SE	Ascorbic acid	
1000	88.5 ± 0.004	97.5 ± 0.041	1.002
500	79.7 ± 0.007	94.4 ± 0.023	0.921
250	71.7 ± 0.020	92.8 ± 0.001	1.032
125	64.4 ± 0.031	90.3 ± 0.036	1.332
62.5	57.3 ± 0.005	83.4 ± 0.004	2.032
31.25	49.9 ± 0.003	75.2 ± 0.006	2.154
15.625	41.9 ± 0.041	66.9 ± 0.002	1.031
7.8125	33.7 ± 0.003	57.4 ± 0.015	2.321
3.9	24.5 ± 0.008	49.8 ± 0.003	1.012
1.95	16.4 ± 0.015	44.2 ± 0.005	2.21
0	0.0	0.0	000
IC_{50} (µg/mL)	34.51 ± 1.46	2.82 ± 0.79d	2.10

Cytotoxic Activity

The MTT assay was used to examine the biocompatibility activities of NC ZnO/CuO/Se against Wi38 (normal cell lines) cells. The findings in Table 4 and Fig. 5 showed that normal cell line proliferation was inversely correlated with concentration, with low concentrations increasing viability or proliferation and *vice versa*. At a high concentration (1000 µg mL^{-1}), the viability of cell lines was 7.09 ± 0.65%. At low concentrations, the viability percentages rose. For example, at 125 and 250 µg mL^{-1}, the Wi38 viability was 99.86 ± 1.25% and 98.11 ± 0.48%, respectively. According to the statistical evaluation, the synthesized NC ZnO/CuO/Se's IC_{50} values for Wi83 were 593.08 ± 2.35. According to the results, normal cells were less harmed by high levels of the generated nanoalloy (500 and 250 µg mL^{-1}). In other words, normal cells can tolerate a high concentration of NC ZnO/CuO/Se. In a different investigation of Se/ZnO/CuO NPs mediated by *Nitraria retusa*, the IC_{50} value was 294.9 ± 4.4 µg mL^{-1} *versus* normal cell lines (WI38) (Amin *et al* 2025). It means that *Schinus terebinthifolia* leaves aqueous extract produced NC ZnO/CuO/Se is more suitable for preparing Se/ZnO/CuO NPs.

Table 4. Effect of NC ZnO/CuO/Se on Wi38 Cells Cytotoxicity and Viability at Different Concentrations

Parameter	Concentration (µg/mL)					
	1000	500	250	125	62.5	31.25
Viability %	7.09 ± 0.65	48.38 ± 1.01	98.11 ± 0.48	99.86 ± 1.25	99.95 ± 0.42	99.95 ± 1.01
Toxicity %	92.90 ± 0.25	51.61 ± 0.54	1.88 ± 0.09	0.14 ± 0.02	0.05 ± 0.01	0.05 ± 0.01
IC_{50} (µg/mL)	593.08 ± 2.35					

Lipase Inhibition

A common way of drug development is the screening of lipase inhibitors from natural compounds, as there is a considerable need for new anti-obesity medications to treat obesity. In this study (Fig. 6), the biogenic NC ZnO/CuO/Se at doses from 1.95 to 1000 ug/mL exhibited excellent enzyme inhibition potential ranging from 12.2 to 90.4% respectively, with IC50 = 41.66 ug/mL against lipase.

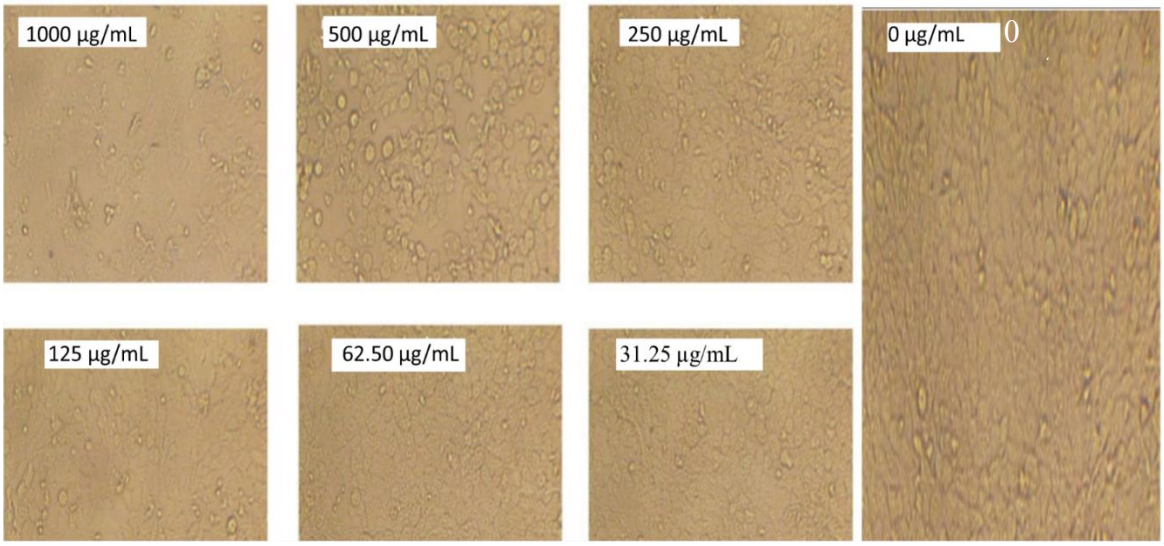

Fig. 5. Effect of different concentrations of NC ZnO/CuO/Se on Wi38 cells

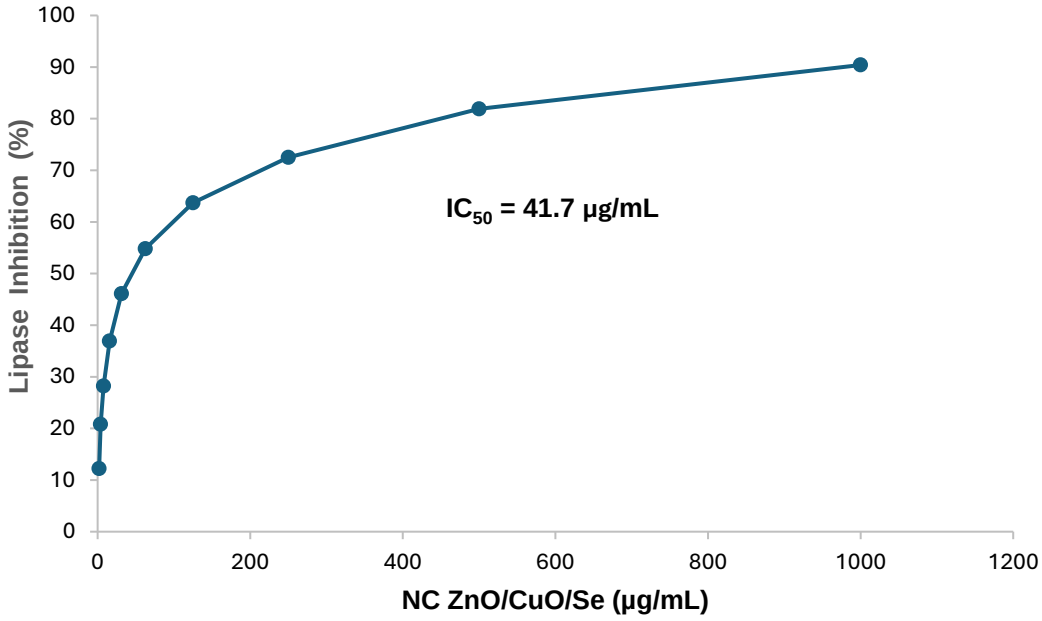

Fig. 6. Effect of NC ZnO/CuO/Se on lipase activity at different concentrations

A report on CuO-NPs at 200 µg /mL has a percent inhibition of lipase at 80.5% (Iqbal *et al*. 2022). The phytochemicals and functional molecules as carbonyl group (C-O)

and hydroxyl group (OH^-) conjugated to NC ZnO/CuO/Se during the biosynthesis process may be the cause of the inhibitory impact (Islam *et al*. 2017). According to these data, these NPs can be used to treat *H pylori* and obesity theaters.

CONCLUSIONS

1. *Schinus terebinthifolia* leaves offer a safe and efficient method for creating ZnO/CuO/Se nanocomposite without endangering the environment.
2. The Fourier transform infrared (FTIR), X-ray diffraction (XRD), scanning electron microscopy with energy dispersive X-range spectroscopy (SEM-EDX), transmission electron microscopy (TEM), and selected area electron diffraction (SAED) analysis presented functional groups that share in the formation of NC ZnO/CuO/Se. Additionally, the size of NC ZnO/CuO/Se ranged from 40 to 50 nm.
3. The NC ZnO/CuO/Se showed antibacterial and antibiofilm efficacy against *H. pylori.*
4. High antioxidant qualities were demonstrated by the NC ZnO/CuO/Se (> 88% in the DPPH assay).
5. The NC ZnO/CuO/Se demonstrated outstanding enzyme inhibition capacity against lipase, with an IC50 of 41.7 ug/mL.
6. Furthermore, cytotoxicity assessment showed low cytotoxicity of NPs at high concentrations against normal cells.

ACKNOWLEDGMENTS

The authors wish to acknowledge Princess Nourah bint Abdulrahman University Researchers Supporting Project number (PNURSP2025R217), Princess Nourah bint Abdulrahman University, Riyadh, Saudi Arabia.

Funding

This research was funded by Princess Nourah bint Abdulrahman University Researchers Supporting Project number (PNURSP2025R217), Princess Nourah bint Abdulrahman University, Riyadh, Saudi Arabia

REFERENCES CITED

Abdelghany, T. M., Al-Rajhi, A. M. H., Yahya, R., Bakri, M. M., Al Abboud, M. A., Yahya, R., and Salem, S. S. (2023b). "Phytofabrication of zinc oxide nanoparticles with advanced characterization and its antioxidant, anticancer, and antimicrobial activity against pathogenic microorganisms," *Biomass Conversion and Biorefinery* 13, 417-430. DOI: 10.1007/s13399-022-03412-1

Abdelghany, T. M., Al-Rajhi, A. M., Almuhayawi, M. S., Abada, E., Al Abboud, M. A., Moawad, H., and Selim, S. (2023a). "Green fabrication of nanocomposite doped with

selenium nanoparticle–based starch and glycogen with its therapeutic activity: Antimicrobial, antioxidant, and anti-inflammatory in vitro," *Biomass Conversion and Biorefinery* 13(1), 431-443. DOI: 10.1007/s13399-022-03257-8

Aborabu, A. A., Tayel, A. A., Assas, M., Moussa, S. H., Alalawy, A. I., Almutairi, F. M., and Omar, A. A. (2024). "Anti-*Helicobacter pylori* activity of nanocomposites from chitosan/broccoli mucilage/selenium nanoparticles," *Scientific Reports* 14(1), article ID 21693. DOI: 10.1038/s41598-024-65762-2

Alghonaim, M. I., Alsalamah, S. A., Mohammad, A. M., and Abdelghany, T. M. (2024). "Green synthesis of bimetallic Se@ TiO_2NPs and their formulation into biopolymers and their utilization as antimicrobial, anti-diabetic, antioxidant, and healing agent *in vitro*," *Biomass Conversion and Biorefinery* 15, 6767-6779. DOI: 10.1007/s13399-024-05451-2

Al-Rajhi A. M. H., and Abdelghany T. M. (2023a). "*In vitro* repress of breast cancer by bio-product of edible *Pleurotus ostreatus* loaded with chitosan nanoparticles," *Applied Biology & Chemistry* 66, article 33. DOI: 10.1186/s13765-023-00788-0

Al-Rajhi, A. M. H., and Abdelghany, T. M. (2023b). "Nanoemulsions of some edible oils and their antimicrobial, antioxidant, and anti-hemolytic activities," *BioResources* 18(1), 1465-1481. DOI: 10.15376/biores.18.1.1465-1481

Al-Rajhi, A. M. H., Qanash, H., Almashjary, M. N., Hazzazi, M. S., Felemban, H. R., and Abdelghany, T. M. (2023a). "Anti-*Helicobacter pylori*, antioxidant, antidiabetic, and anti-alzheimer's activities of laurel leaf extract treated by moist heat and molecular docking of its flavonoid constituent, naringenin, against acetylcholinesterase and butyrylcholinesterase," *Life* 13(7), article 1512. DOI: 10.3390/life13071512

Al-Rajhi, A. M. H., Qanash, H., Bazaid, A. S., Binsaleh, N. K., and Abdelghany, T. M. (2023b). "Pharmacological evaluation of *Acacia nilotica* flower extract against *Helicobacter pylori* and human hepatocellular carcinoma *in vitro and in silico*," *Journal of Functional Biomaterials* 14(4), article 237. DOI: 10.3390/jfb14040237

Al-Rajhi, A. M. H., Yahya, R., Bakri, M. M. Y. R., and Abdelghany, T. M. (2022). "*In situ* green synthesis of Cu-doped ZnO based polymers nanocomposite with studying antimicrobial, antioxidant and anti-inflammatory activities," *Applied Biological Chemistry* 65, article 35. DOI: 10.1186/s13765-022-00702-0

Amin, M. A. A., Abu-Elsaoud, A. M., Nowwar, A. I., Abdelwahab, A. T., Awad, M. A., Hassan, S. E. D., and Elkelish, A. (2024). "Green synthesis of magnesium oxide nanoparticles using endophytic fungal strain to improve the growth, metabolic activities, yield traits, and phenolic compounds content of *Nigella sativa* L.," *Green Processing and Synthesis* 13(1), article ID 20230215. DOI: 10.1515/gps-2023-0215

Amin, M. A., Algamdi, N. A., Waznah, M. S., Bukhari, D. A., Alsharif, S. M., Alkhayri, F., Abdel-Nasser, M., and Fouda, A. (2025). "An insight into antimicrobial, antioxidant, anticancer, and antidiabetic activities of trimetallic Se/ZnO/CuO nanoalloys fabricated by aqueous extract of *Nitraria retusa*," *Journal of Cluster Science* 36(1), article 19. DOI: 10.1007/s10876-024-02742-6

Bakri, M. M., Alghonaim, M. I., Alsalamah, S. A., Yahya, R. O., Ismail, K. S., and Abdelghany, T. M. (2024). "Impact of moist heat on phytochemical constituents, anti-*Helicobacter pylori*, antioxidant, anti-diabetic, hemolytic and healing properties of

rosemary plant extract *in vitro*," *Waste and Biomass Valorization* 15, 4965-4979. DOI: 10.1007/s12649-024-02490-8

Bjerregaard, L. G., Jensen, B. W., Ängquist, L., Osler, M., Sørensen, T. I., and Baker, J. L. (2018). "Change in overweight from childhood to early adulthood and risk of type 2 diabetes," *New England Journal of Medicine* 378(14), 1302-1312. DOI: 10.1056/NEJMoa1713231

Cao, Y., Dhahad, H. A., El-Shorbagy, M. A., Alijani, H. Q., Zakeri, M., Heydari, A., Bahonar, E., Slouf, M., Khatami, M., and Dehkordi, F. F. (2021). "Green synthesis of bimetallic ZnO–CuO nanoparticles and their cytotoxicity properties," *Scientific Reports* 11(1), article 23479. DOI: 10.1038/s41598-021-02937-1

Castillo-Juárez, I., Rivero-Cruz, F., Celis, H., and Romero, I. (2007). "Anti-*Helicobacter pylori* activity of anacardic acids from *Amphipterygium adstringens*," *Journal of Ethnopharmacology* 114(1), 72-77. DOI: 10.1016/j.jep.2007.07.022

da Silva Nascimento, M., Dos Santos, P. H., de Abreu, F. F., Shan, A. Y., Amaral, R. G., Andrade, L. N., Andrade, L. N., Souto, E. B., Santos, M. I. S., Graça, A. S., *et al*. (2023). "*Schinus terebinthifolius* Raddi (*Brazilian pepper*) leaves extract: *In vitro* and *in vivo* evidence of anti-inflammatory and antioxidant properties," *Inflammopharmacology* 31(5), 2505-2519. DOI: 10.1007/s10787-023-01316-8

Dobrucka, R. (2020). "Biogenic synthesis of trimetallic nanoparticles Au/ZnO/Ag using *Meliloti officinalis* extract," *International Journal of Environmental Analytical Chemistry* 100(9), 981-991. DOI: 10.1080/03067319.2019.1646736

El-Batal, A. I., Ismail, M. A., Amin, M. A., El-Sayyad, G. S., and Osman, M. S. (2023). "Selenium nanoparticles induce growth and physiological tolerance of wastewater-stressed carrot plants," *Biologia* 78(9), 2339-2355. DOI: 10.1007/s11756-023-01401-x

Fahim, Y. A., El-Khawaga, A. M., Sallam, R. M., Elsayed, M. A., and Assar, M. F. A. (2024). "A review on lipases: Sources, assays, immobilization techniques on nanomaterials and applications," *BioNanoScience* 14, 1780-1797. DOI: 10.1007/s12668-024-01319-x

French, G. L. (2006). "Bactericidal agents in the treatment of MRSA infections – The potential role of daptomycin," *Journal of Antimicrobial Chemotherapy* 58(6), 1107-1117. DOI: 10.1093/jac/dkl393

Hasanin, M. S., and Youssef, A. M. (2022). "Ecofriendly bioactive film doped CuO nanoparticles based biopolymers and reinforced by enzymatically modified nanocellulose fibers for active packaging applications," *Food Packaging and Shelf Life* 34, article 100979. DOI: 10.1016/j.fpsl.2022.100979

Hashem, A. H., Al-Askar, A. A., Haponiuk, J., Abd-Elsalam, K. A., and Hasanin, M. S. (2023). "Biosynthesis, characterization, and antifungal activity of novel trimetallic copper oxide–selenium–zinc oxide nanoparticles against some mucorales fungi," *Microorganisms* 11(6), article ID 1380. DOI: 10.3390/microorganisms11061380

He, C., Hu, Y., Yin, L., Tang, C., and Yin, C. (2010). "Effects of particle size and surface charge on cellular uptake and biodistribution of polymeric nanoparticles," *Biomaterials* 31(13), 3657-3666. DOI: 10.1016/j.biomaterials.2010.01.065

Hooi, J. K. Y., Lai, W. Y., Ng, W. K., Suen, M. M. Y., Underwood, F. E., Tanyingoh, D., Malfertheiner, P., Graham, D. Y., Wong, V. W. S., Wu, J. C. Y., Chan, F. K. L., Sung, J. J. Y., Kaplan, G. G., and Ng, S. C. (2017). "Global prevalence of *Helicobacter pylori*

infection: Systematic review and meta-analysis," *Gastroenterology* 153(2), 420-429. DOI: 10.1053/j.gastro.2017.04.022

Idris, D. S., Roy, A., Malik, A., Khan, A. A., Sharma, K., and Roy, A. (2025). "Green synthesis of silver oxide-nickel oxide bimetallic nanoparticles using peels of *Citrus sinensis* and their application," *Journal of Inorganic and Organometallic Polymers and Materials* 35(1), 594-606. DOI: 10.1007/s10904-024-03316-9

Iqbal, J., Andleeb, A., Ashraf, H., Meer, B., Mehmood, A., Jan, H., Zaman, G., Nadeem, M., Drouet, S., Fazal, H., *et al.* (2022). "Potential antimicrobial, antidiabetic, catalytic, antioxidant and ROS/RNS inhibitory activities of *Silybum marianum* mediated biosynthesized copper oxide nanoparticles," *RSC Advances* 12(22), 14069-14083.

Islam, N. U., Amin, R., Shahid, M., Amin, M., Zaib, S., and Iqbal, J. (2017). "A multi-target therapeutic potential of *Prunus domestica* gum stabilized nanoparticles exhibited prospective anticancer, antibacterial, urease-inhibition, anti-inflammatory and analgesic properties," *BMC Complementary and Alternative Medicine* 17, article 276. DOI: 10.1186/s12906-017-1791-3

Kunwar, S., Roy, A., Bhusal, U., Gacem, A., Abdullah, M. M., Sharma, P., Yadav, K. K., Rustagi, S., Chatterjee, N., Deshwal, V. K., *et al.* (2023). "Bio-fabrication of Cu/Ag/Zn nanoparticles and their antioxidant and dye degradation activities," *Catalysts* 13(5), article 891. DOI: 10.3390/catal13050891

Malm, A., Glowniak-Lipa, A., Korona-Glowniak, I., and Baj, T. (2015). "Anti-*Helicobacter pylori* activity *in vitro* of chamomile flowers, coneflower herbs, peppermint leaves and thyme herbs–a preliminary report," *Current Issues in Pharmacy and Medical Sciences* 28(1), 30-32. DOI: 10.1515/cipms-2015-0038

Michael, A., Singh, A., Mishra, R., Roy, A., Roy, A., Kaur, K., Rustagi, S., Malik, S., Verma, R., and Sharma, K. (2024). "Biogenic synthesis of silver nanoparticles from Solanum tuberosum peel and their potent antibacterial action," *Nano-Structures & Nano-Objects* 38, article 101190. DOI:10.1016/j.nanoso.2024.101190

Naiel, B., Fawzy, M., Halmy, M. W. A., and Mahmoud, A. E. D. (2022). "Green synthesis of zinc oxide nanoparticles using sea lavender (*Limonium pruinosum* L. Chaz.) extract: Characterization, evaluation of anti-skin cancer, antimicrobial and antioxidant potentials," *Scientific Reports* 12(1), article ID 20370. DOI: 10.1038/s41598-022-24805-2

Nasrollahzadeh, M., Sajjadi, M., Iravani, S., and Varma, R. S. (2020). "Trimetallic nanoparticles: Greener synthesis and their applications," *Nanomaterials* 10(9), article ID 1784. DOI: 10.3390/nano10091784

Paul, D., Mangla, S., and Neogi, S. (2020). "Antibacterial study of CuO-NiO-ZnO trimetallic oxide nanoparticle," *Materials Letters* 271, article ID 127740. DOI: 10.1016/j.matlet.2020.127740

Peddi, P., Ptsrk, P. R., Rani, N. U., and Tulasi, S. L. (2021). "Green synthesis, characterization, antioxidant, antibacterial, and photocatalytic activity of *Suaeda maritima* (L.) Dumort aqueous extract-mediated copper oxide nanoparticles," *Journal of Genetic Engineering and Biotechnology* 19(1), article 131. DOI: 10.1186/s43141-021-00229-9

Qanash, H., Al-Rajhi, A. M. H., Almashjary, M. N., Basabrain, A. A., Hazzazi, M. S., and Abdelghany, T. M. (2023a). "Inhibitory potential of rutin and rutin nano-crystals

against *Helicobacter pylori*, colon cancer, hemolysis and Butyrylcholinesterase *in vitro* and *in silico*," *Applied Biology and Chemistry* 66, article 79. DOI: 10.1186/s13765-023-00832-z

Qanash, H., Bazaid, A. S., Aldarhami, A., Alharbi, B., Almashjary, M. N., Hazzazi, M. S., Felemban, H. R., and Abdelghany, T. M. (2023b). "Phytochemical characterization and efficacy of *Artemisia judaica* extract loaded chitosan nanoparticles as inhibitors of cancer proliferation and microbial growth," *Polymers* 15(2), article 391. DOI: 10.3390/polym15020391

Revathi, S., Dey, N., Thangaleela, S., Vinayagam, S., Gnanasekaran, L., Sundaram, T., Malik, A., Khan, A. A., Roy, A., and Kumar, A. (2024). "Nanocarrier optimization: encapsulating *Hydrastis canadensis* in chitosan nanoparticles for enhanced antibacterial and dye degradation performance," *International Journal of Biological Macromolecules* 274, article 133316. DOI: 10.1016/j.ijbiomac.2024.133316

Roh, C., and Jung, U. (2012). "Screening of crude plant extracts with anti-obesity activity," *International Journal of Molecular Sciences* 13(2), 1710-1719. DOI: 10.3390/ijms13021710

Salama, A. M., Helmy, E. A., Abd El-ghany, T. M., and Ganash M. (2021). "Nickel oxide nanoparticles application for enhancing biogas production using certain wastewater bacteria and aquatic macrophytes biomass," *Waste Biomass Valor* 12, 2059–2070 . DOI: 10.1007/s12649-020-01144-9

Sánchez, J., Priego, T., Palou, M., Tobaruela, A., Palou, A., and Picó, C. (2008). "Oral supplementation with physiological doses of leptin during lactation in rats improves insulin sensitivity and affects food preferences later in life," *Endocrinology* 149(2), 733-740. DOI: 10.1210/en.2007-0630

Sasaki, Y., Abe, Y., Shoji, M., Mizumoto, N., Takeda, H., Oizumi, H.,Yaoita, T., Sawada, N., Yamagishi, K., Saito, K. E., *et al.* (2021). "Reliability of self-reported questionnaire for epidemiological investigation of *Helicobacter pylori* eradication in a population-based cohort study," *Scientific Reports* 11(1), article ID 15605. DOI: 10.1038/s41598-021-95124-1

Selim, S., Alruwaili, Y., Ejaz, H., Abdalla, A. E., Almuhayawi, M. S., Nagshabandi, M. K., and Abdelghany, T. M. (2024). "Estimation and action mechanisms of cinnamon bark via oxidative enzymes and ultrastructures as antimicrobial, anti-biofilm, antioxidant, anti-diabetic, and anticancer agents," *BioResources* 19(4), 7019-7041. DOI: 10.15376/biores.19.4.7019-7041

Selim, S., Saddiq, A. A., Ashy, R. A., Baghdadi, A. M., Alzahrani, A. J., Mostafa, E. M., Al Jaouni, S. K., Elamir, M. Y. M., Amin, M. A., and Hagagy, N. (2025b). "Bimetallic selenium/zinc oxide nanoparticles: Biological activity and plant biostimulant properties," *AMB Express* 15(1), article 1. DOI: 10.1186/s13568-024-01808-y

Shehab, W. S., Elsayed, D. A., Abdel Hamid, A. M., Assy, M. G., Mouneir, S. M., Hamed, E. O., Mousa, S. M., and El-Bassyouni, G. T. (2024). "CuO nanoparticles for green synthesis of significant anti-*Helicobacter pylori* compounds with *in silico* studies," *Scientific Reports* 14(1), article 1608. DOI: 10.1038/s41598-024-51708-1

Shirani, M., Pakzad, R., Haddadi, M. H., Akrami, S., Asadi, A., Kazemian, H., Moradi, M., Kaviar, V. H., Zomorodi, A. R., Khoshnood, S., Shafieian, M., Tavasolian, R., Heidary, M., and Saki, M. (2023). "The global prevalence of gastric cancer in

Helicobacter pylori-infected individuals: a systematic review and meta-analysis," *BMC Infect Dis*. 23(1), 543. DOI: 10.1186/s12879-023-08504-5

Singh, V., Pandit, C., Pandit, S., Roy, A., Rustagi, S., Awwad, N. S., Ibrahium, H. A., Anand, J., Malik, S., Yadav, K. K., and Tambuwala, M. (2024). "Deciphering the mechanisms and biotechnological implications of nanoparticle synthesis through microbial consortia," *Journal of Basic Microbiology* 64(10), article e2400035. DOI: 10.1002/jobm.202400035

Soliman, M. K., Amin, M. A. A., Nowwar, A. I., Hendy, M. H., and Salem, S. S. (2024). "Green synthesis of selenium nanoparticles from *Cassia javanica* flowers extract and their medical and agricultural applications," *Scientific Reports* 14(1), article 26775. DOI: 10.1038/s41598-024-77353-2

Surendra, B. S., Mallikarjunaswamy, C., Pramila, S., and Rekha, N. D. (2021). "Bio-mediated synthesis of ZnO nanoparticles using lantana camara flower extract: Its characterizations, photocatalytic, electrochemical and anti-inflammatory applications," *Environmental Nanotechnology, Monitoring & Management* 15, article 100442. DOI: 10.1016/j.enmm.2021.100442

Yahya, R., Al-Rajhi, A. M. H., Alzaid, S. Z., Al Abboud, M. A., Almuhayawi, M. S., Al Jaouni, S. K., and Abdelghany, T. M. (2022). "Molecular docking and efficacy of *Aloe vera* gel based on chitosan nanoparticles against *Helicobacter pylori* and its antioxidant and anti-inflammatory activities," *Polymers* 14(15), article 2994. DOI: 10.3390/POLYM14152994

Article submitted: February 24, 2025; Peer review completed: March 29, 2025; Revised version received: April 5, 2025; Further revised version received and accepted: April 8, 2025; Published: April 25, 2025.
DOI: 10.15376/biores.20.2.4432-4449